
Article:
Dogan, H., Sims, N.D. orcid.org/0000-0002-6292-6736 and Wagg, D.J. orcid.org/0000-0002-7266-2105 (2019) Investigation of the inerter-based dynamic vibration absorber for machining chatter suppression. Journal of Physics: Conference Series, 1264. 012030. ISSN 1742-6588

https://doi.org/10.1088/1742-6596/1264/1/012030

Investigation of the inerter-based dynamic vibration absorber for machining chatter suppression

IOP Conf. Series: Journal of Physics: Conf. Series **1264** (2019) 012030 doi:10.1088/1742-6596/1264/1/012030

Investigation of the inerter-based dynamic vibration absorber for machining chatter suppression

Hakan Dogan, Neil D Sims and David J Wagg

Department of Mechanical Engineering, University of Sheffield, S1 3JD, UK

E-mail: hdogan1@sheffield.ac.uk, n.sims@sheffield.ac.uk, david.wagg@sheffield.ac.uk

Abstract. This study proposes a novel approach to increase the chatter stability in machining operations. It shows the potential performance improvement when an inerter-based dynamic vibration absorber is employed in a machining operation. Tuned inerter based devices have been employed to decrease the magnitude of the vibrations in applications such as civil engineering structures and vehicle suspension systems but the nature of chatter in machining is different from these applications. Therefore, it requires a different tuning methodology to obtain the optimal design parameters. In this study, the machining operation is modelled as an undamped single degree of freedom system and different configurations of an inerter, a damper and two springs are used to ensure a stable region of operation. Strategies for the tuning parameters are developed both analytically and numerically. Using these techniques the performance improvement in the chatter stability provided by using inerter based devices instead of a traditional dynamic vibration absorber is demonstrated.

1. Introduction

Regenerative chatter can be seen as one of the biggest issues in machining processes, and can be defined as undesired vibrations between the workpiece and cutting tool. It causes poor surface finish and reduces productivity. Also, chatter leads to fast tool wear (or even tool breakage) which shortens the life cycle of the tool. Therefore, it is important to have a chatter-free operation to increase productivity.

Dynamic vibration absorbers have been widely used to increase the chatter performance of machining operations due to their simplicity, low cost and reliability. Tarng et al. [1] demonstrated that a piezoelectric vibration absorber can improve the chatter stability by matching the natural frequency of the absorber with the structure's target mode. Moradi et al. [2] presented chatter stability improvement by investigating the position of a tunable vibration absorber along a boring bar in a turning operation. More sophisticated designs such as nonlinear, two-degree-of-freedom and multiple tuned mass dampers have been proposed to suppress chatter vibrations [3–6]. Also, active vibration absorbers have been investigated to improve chatter performance [7, 8]. Although active vibration absorbers tend to offer more performance improvement, they are more complex, expensive and difficult to implement than passive vibration absorbers.

The use of a relative-acceleration-dependent inertial mechanism, alongside the stiffness and the damping components, was already proposed by Kuroda et al. [9] and Saito et al. [10] in order to increase the limited performance of an absorber system. Similarly, the inerter, first defined by

Smith [11], provides an inertial force proportional to the a relative acceleration at its terminals. Recently, inerter based devices have been investigated to improve performances of the vibratory systems. Wang et al. [12] studied the building suspension design with inerters and Lazar et al. [13] employed an inerter based device for structural vibration suppression. Inerter based devices were also tested for railway vehicles [14] and vehicle suspension systems [15,16]. Recently, Wang and Lee [17] proposed to utilize an inerter to increase vibration suppression of milling machine tools. However, they focused on the amplitude of the displacement of the vibration rather than the chatter stability. Furthermore, the suspension network that was proposed in the study did not operate with a proof-mass but instead required a mechanical connection to a rigid body, which limits its practical use.

Tuning parameters are crucial to obtain the best performance from traditional or inerter-based absorbers. For traditional dynamic vibration absorbers, it is common to use Den Hartog's fixed-points method [18] to set the parameters of the components of the absorber. However, this method does not give the optimum parameters for a machining operations since machining chatter stability is related to the real part of the frequency response function (FRF). Therefore, an analytical tuning strategy, which focuses on the real part of the FRF, was developed by Sims [19]. Both analytical strategies developed by Den Hartog and Sims are valid if the primary system of interest is undamped. Numerical optimisation methods can be used for optimisation of damped systems [6, 20, 21]. H_2 and H_∞ performances of six different configurations of inerter-based dynamic vibration absorbers were evaluated by Hu et al. [22] using a numerical optimisation method. Also, closed-form solutions for the optimal parameters of inerter-based dynamic vibration absorbers have been recently obtained by Barredo et al. [23]. Still, the focus of this study was the amplitude of the displacement of the vibration instead of the real part of the FRF, which is more related to machining chatter stability.

This study will investigate four different layouts of the inerter-based dynamic vibration absorber to improve machining chatter stability. The tuning strategies will be evaluated both analytically and numerically. After finding the optimal design parameters for the configurations, the performance evaluation will be made and a conclusion will be drawn.

2. Machining dynamics

For machining, it is crucial to understand the regenerative effect underlying chatter. In that way, the inverse proportional relationship between the limiting depth of cut and the real part of the FRF can be demonstrated and a tuning strategy can be developed. We consider a machining process that can be described as a turning operation in the following way. Due to undulations on the surface of the workpiece, the instantaneous chip thickness can be written as

$$h(t) = h_m + y(t - T) - y(t) \tag{1}$$

where h_m is the intended chip thickness, $y(t - T)$ is the displacement of the vibration due to the previous cut and $y(t)$ is the displacement of the vibration due to the current cut as seen in Figure 1. T is the time delay because of the workpiece rotation.

The cutting force can be derived by considering only the y-direction

$$F(t) = b_{cut} K_s h(t) \tag{2}$$

where b_{cut} and K_s are the depth of cut and specific cutting force coefficient, respectively. The multiplication of b_{cut} and $h(t)$ gives the chip area removed from the workpiece and K_s defines the interaction between the cutting tool and the workpiece. Taking the Laplace Transform of Equation 1 and Equation 2 gives

$$F(s) = b_{cut} K_s h(s) \tag{3}$$

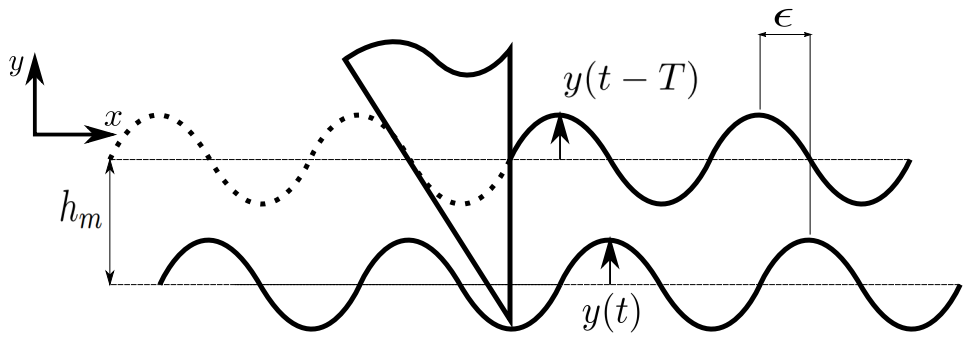

Figure 1. The undulations due to the current and previous cuts

$$h(s) = h_m(s) + y(s)(e^{-sT} - 1) \tag{4}$$

and the output can be written as the product of the transfer function and the input,

$$y(s) = G(s)F(s) = G(s)b_{cut}K_s h(s) \tag{5}$$

where $G(s)$ is the transfer function of the cutting tool-workpiece system. Substituting Equation 4 into Equation 3 yields

$$\frac{h(s)}{h_m(s)} = \frac{1}{1 + (1 - e^{-sT})K_s b_{cut} G(s)} \tag{6}$$

The stability analysis of Equation 6 gives

$$1 + (1 - e^{-sT})K_s b_{lim} G(s) = 0 \tag{7}$$

as the condition for the limit of stability. For the frequency domain, $s = j\omega_c$ and $e^{-j\omega_c T} = \cos\omega_c T - j\sin\omega_c T$ can be written. Therefore,

$$\begin{aligned} &1 + K_s b_{lim}(\Re\{G(s)\} - \Re\{G(s)\}cos(\omega_c T) - \Im\{G(s)\}sin(\omega_c T)) \\ &+jK_s b_{lim}(\Im\{G(s)\} + \Re\{G(s)\}sin(\omega_c T) - \Im\{G(s)\}cos(\omega_c T)) = 0 \end{aligned} \tag{8}$$

When the real part and imaginary part of Equation 8 are evaluated separately, these expressions can be found:

$$\omega_c T = 3\pi + 2\psi \tag{9}$$

$$b_{lim} = -\frac{1}{2K_s \Re\{G(\omega_c)\}} \tag{10}$$

where b_{lim} is the limit of depth of cut and defines the stability boundary. ω_c is chatter frequency at which the workpiece oscillates, $\psi = tan^{-1}\frac{\Im\{G(\omega_c)\}}{\Re\{\omega_c\}}$ is the phase angle of the structure and $\omega_c T = \epsilon$ is the phase shift between inner and outer modulations (waviness at current and previous cuts). The number of vibration waves left on the workpiece is given by

$$\frac{\omega_c}{2\pi} T = k + \frac{\epsilon}{2\pi} \tag{11}$$

where k is the integer number of waves and $\frac{\epsilon}{2\pi}$ is the fraction of the redundant wave. In the case of $\epsilon = 0$, there is no fractional wave and two consecutive cuts are in phase.

Equation 10 demonstrates that the limiting depth of cut is inversely proportional to the negative real part of the FRF of the system. This means that a smaller absolute value of the most negative real value indicates an improvement in the chatter performance. Hence, the tuning strategy must focus on the absolute value of the most negative real value to make it as small as possible. In the following section, the mathematical model and the displacement transfer function will be presented in order to conduct simulations.

3. Mathematical model of the system

Six different configurations of inerter-based dynamic vibration absorbers were investigated for H_∞ and H_2 by Hu et al. [22]. Their study has already shown that there is no benefit to add an inerter to traditional dynamic vibration absorber (e.g. configurations C1 and C2 in [22]). Also, it has been demonstrated that an inerter and an additional spring added to a traditional dynamic vibration absorber (e.g. configurations C3-C6 in [22]) improves the H_∞ and H_2 performances of the absorbers. The question that is considered in the present study is whether these four configurations can increase the chatter stability in a machining operation. The four configurations and their transfer function representations are first defined in this section.

A machining system with an inerter-based dynamic vibration absorber can be modelled as seen in Figure 2. The displacement transfer function can be derived as [22]

$$H(s) = \frac{x}{x_s} = \frac{1}{\frac{s^2}{\omega_n^2} + \frac{1}{K}R(s) + 1} \tag{12}$$

where

$$R(s) = \frac{(k + sY(s))ms^2}{k + ms^2 + sY(s)} \tag{13}$$

and where $x_s = \frac{F}{K}$ and $\omega_n = \sqrt{\frac{K}{M}}$ are the static displacement and natural frequency of the machining system. The displacement transfer function is $H(s) = KG(s)$ so the transfer function of the cutting tool-workpiece system can be obtained easily. $Y(s)$ is the impedance of the inerter-based device and varies depending on the configurations which are given in Figure 3. The impedance for each configuration is also presented in Table 1.

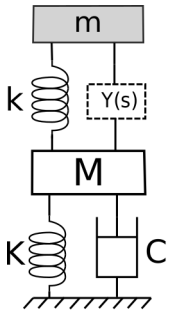

Figure 2. Inerter-based dynamic vibration absorber

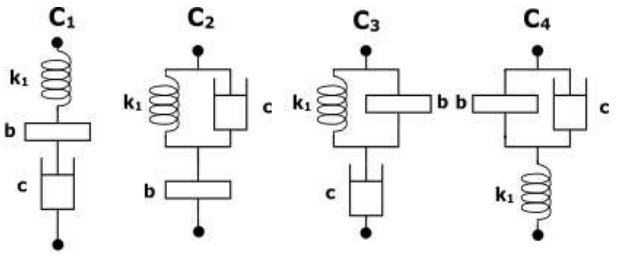

Figure 3. Four configurations investigated in this study

The displacement frequency response function can be defined by replacing s with $j\omega$ in Equation 12 in the form of

$$H_i(j\lambda) = \frac{R_{ni} + jI_{ni}}{R_{di} + jI_{di}}, \quad i = 1, ..., 4 \tag{14}$$

by using the following non-dimensional terms

Table 1. Impedance for each configuration in Figure 3

$$Y_1(s) = \frac{1}{\frac{s}{k_1}+\frac{1}{c}+\frac{1}{bs}} \qquad Y_2(s) = \frac{1}{\frac{1}{\frac{k_1}{s}+c}+\frac{1}{bs}}$$

$$Y_3(s) = \frac{1}{\frac{1}{\frac{k_1}{s}+bs}+\frac{1}{c}} \qquad Y_4(s) = \frac{1}{\frac{1}{bs+c}+\frac{s}{k1}}$$

$$\begin{aligned} \text{mass ratio} \quad & \mu = \frac{m}{M} \\ \text{inertance-to-mass ratio} \quad & \delta = \frac{b}{m} \\ \text{damping ratio} \quad & \zeta = \frac{c}{2\sqrt{mk}} \\ \text{corner frequency ratio} \quad & \eta = \frac{\omega_b}{\omega_m} \\ \text{natural frequency ratio} \quad & \gamma = \frac{\omega_m}{\omega_n} \\ \text{forced frequency ratio} \quad & \lambda = \frac{\omega}{\omega_n} \end{aligned} \tag{15}$$

where $\omega_m = \sqrt{\frac{k}{m}}$, $\omega_b = \sqrt{\frac{k_1}{b}}$, $\omega_n = \sqrt{\frac{K}{M}}$. The full expression of Equation 14 for each configuration, is given in Appendix A. The next section will present the methods to find the optimal design parameters to obtain the best performances from the configurations.

4. Methodology for tuning parameters

Self-adaptive Differential Evolution algorithm (SaDE) [24] is an quick and effective optimisation method for nonlinear functions and thus, it can be used as a numerical optimization method in this problem. The aim of using a numerical optimisation method is to find the optimum design parameters of the configurations. Hence, maximisation of the most negative real part of the FRF will be sought. However, numerical methods are not as easy as analytical methods to implement. For this reason, even though the closed-form solutions in [23] focus on the amplitude of the displacement of the vibration, they are also employed in this study to test whether any improvement in terms of chatter stability can be provided or not. The closed-form solutions are applied for only the configuration which gives the best improvement.

4.1. Numerical optimisation

The objective of the numerical optimisation is to maximise the minimum negative real part of the FRF. For a specified mass ratio, the optimisation problem can be expressed as

$$max_{\gamma,\zeta,\delta,\eta}\Big(min_{\lambda_n}\big(\Re\{H_i(j\lambda_n)\}\big)\Big), i = 1, ..., 4 \tag{16}$$

The problem is solved by using SaDE [24] and Matlab is employed to apply the optimisation algorithm. SaDE solves the optimisation problems by generating a parameter candidate pool for each generation. It is an effective method since the choice of the learning strategy and the two parameters which have an effect on the performance of the optimisation result are adjusted adaptively in SaDE [24]. For mass ratio $\mu = 0.1$, the optimum design parameters that are obtained via SaDE are given in Table 2.

Table 2. Optimal design parameters for the configurations from SaDE

Configurations/Design parameters	γ	ζ	δ	η
C1	1.0680	0.1657	0.2190	1.0476
C2	1.1082	0.0487	0.1890	0.9066
C3	0.9753	0.2093	1.4925	1.5231
C4	1.0134	0.0624	0.1579	1.2469

4.2. Closed-form solutions

As it will be seen in Section 5, configuration C1 provides the best improvement. Thus, the closed-form solutions which have been found in [23] are also tested. It must be noted that these expressions have not been derived for the real part of the FRF. In spite of this, there is a possibility that an inerter-based dynamic vibration absorber tuned by this method can still provide a better chatter suppression performance than traditional dynamic vibration absorber. Therefore, it might be possible to obtain a better chatter suppression performance, even without the computational effort of the numerical optimisation method, by using the closed-form expression. The main reason for this part of this study is to examine whether this is possible or not. The expressions which give the optimal design parameters for configuration C1 are [23]

$$\begin{aligned} \gamma_{opt,C1} &= \frac{1}{1+\mu} \\ \delta_{opt,C1} &= \frac{2\mu}{1+\mu} \\ \eta_{opt,C1} &= \sqrt{1+\mu} \\ \zeta_{opt,C1} &= \sqrt{\frac{11\mu}{9a_1a_2}} \end{aligned} \tag{17}$$

where

$$a_1 = ((\mu^{9/2} + 7\mu^{7/2} + 16\mu^{5/2} + 14\mu^{3/2} + 4\sqrt{\mu})\sqrt{\mu+4} + \mu^5 + 9\mu^4 + 28\mu^3 + 36\mu^2 + 18\mu + 2)$$
$$a_2 = ((-\mu^{7/2} - 6\mu^{5/2} - 10\mu^{3/2} - 4\sqrt{\mu})\sqrt{\mu+4} + mu^4 + 8\mu^3 + 20\mu^2 + 16\mu + 2)$$

5. Results

The simulations were conducted for the four configurations and the design parameters were chosen as presented in Table 2. A simulation was also conducted for configuration C1 with the optimal design parameters which were found by using closed-form solutions in Section 4.2. The primary mass, the mass ratio μ, the natural frequency of the primary system f_n and the specific cutting coefficient K_s were taken as $1kg$, 0.1, $100Hz$ and $1000N/mm^2$, respectively. The result of a machining operation with a traditional dynamic vibration absorber whose design parameters were tuned by Sims' methodology was taken the benchmark for the analysis.

The improvements in terms of the limiting depth of cut (b_{lim}) which were provided from the different configurations are given in Table 3. Figure 4 presents the negative real part of the FRF of the systems for the four configurations and a traditional dynamic vibration absorber as the interest is the negative real part of the FRF in machining chatter stability. The optimal parameters were obtained from the numerical optimisation method for the four configurations and Sims' methodology for the traditional dynamic vibration absorber. Figure 5 demonstrates the real part of the FRF for two different design parameters which were obtained by the numerical optimisation method and the closed-form solutions in [23] for configuration C1 with the benchmark.

The results show that the best performance is obtained by configuration C1 with the parameters which were found by the numerical optimisation method. Hence, the stability lobe diagram of this case is given in Figure 6 with a comparison with the benchmark.

Table 3. Improvements for each configuration

	DVA	C1	C2	C3	C4
$\Re_{min}\{G(j\lambda)\}$ $[N/m]$	$-4.5573x10^{-06}$	$-3.3217x10^{-06}$	$-3.5165x10^{-06}$	$-3.9780x10^{-06}$	$-3.3255x10^{-06}$
b_{lim} for $\Re_{min}\{G(j\lambda)\}$ $[mm]$	0.1097	0.1505	0.1422	0.1257	0.1504
Improvement (%)	–	37.19	29.63	14.59	37.10

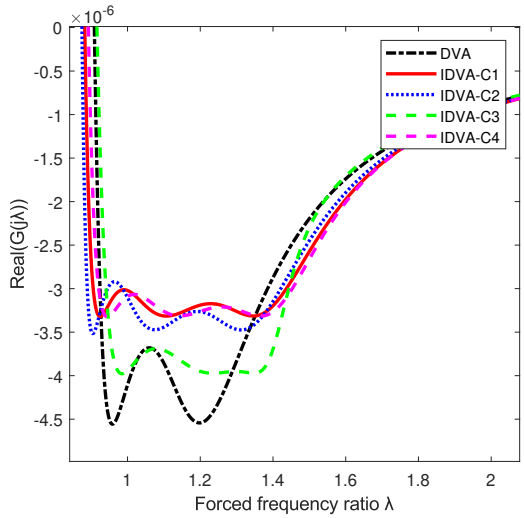

Figure 4. Optimal design parameters results obtained by the numerical optimisation method for C1, C2, C3 and C4, and traditional dynamic vibration absorber result as the benchmark

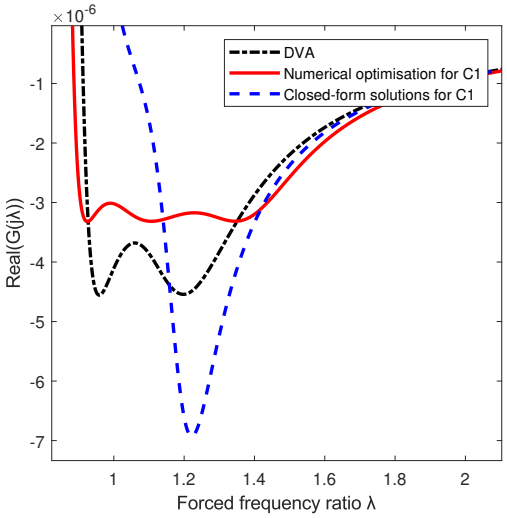

Figure 5. Comparison of the real part of the FRF for different design parameters obtained by the numerical optimisation method and the closed-form solution for configuration C1

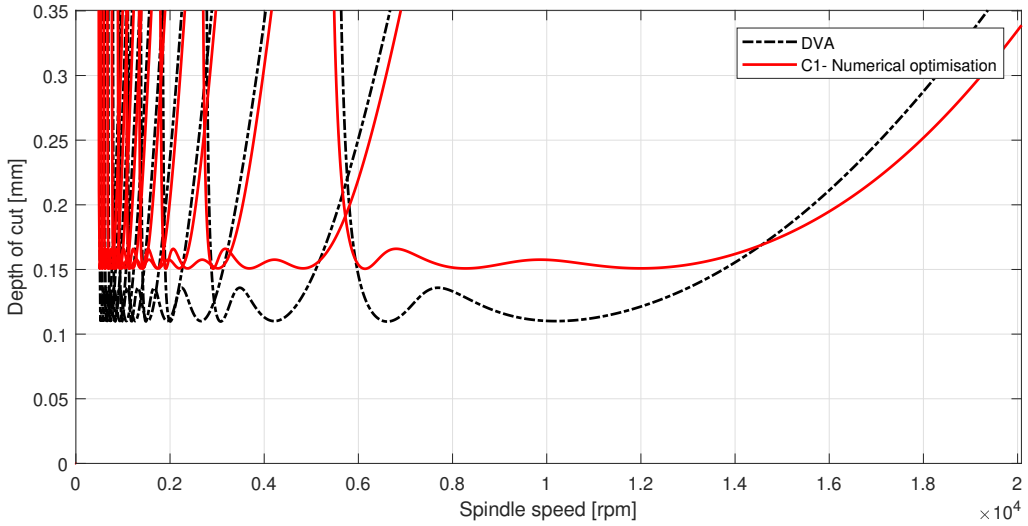

Figure 6. Stability lobe diagram for configuration C1 and traditional dynamic vibration absorber

6. Discussion

The results have shown that the configurations of the inerter-based dynamic vibration absorber studied in this paper can be used to improve machining chatter stability. The best performances have been obtained from configuration C1 (red solid line in Figure 4) and configuration C4 (magenta dashed line in Figure 4) with 37% improvement.

The results have also demonstrated that tuning parameters have a significant effect on the performance of the absorbers as can be seen in Figure 5. The design parameters obtained by using the closed-form solutions in [23] gave a worse performance (blue dashed line in Figure 5) than traditional dynamic vibration absorber (black dashed line in Figure 5) while the design parameters obtained by using the numerical optimisation gave a better performance (red solid line in Figure 5). This is because the closed-form solutions used in the previous study are derived for the magnitude of the displacement of the vibration whereas the performance of the chatter stability is related to the negative real part of the FRF as shown in Equation 10. Thus, the objective function of the numerical optimisation was the real part of the FRF and the design parameters for that case provided significant improvements, especially for configurations C1 and C4.

Although the primary system was assumed to be an undamped system in this study, the numerical optimisation method can also be used to find the optimal design parameters for a damped system, which would be more accurate model for a real machining operation. However, as we are seeking to prove the concept, an undamped model is sufficient for the sake of simplicity. Moreover, the use of an undamped model as a primary system in this study provided the observation of the difference between two tuning methodologies that are adjusted for the amplitude of the displacement of the vibration and the negative real part of the FRF in an analysis of the machining chatter stability. It has been seen that only employment of the inerter is not sufficient to obtain an improvement. The design parameters have a key role in the performance so they must be tuned with the right method.

7. Conclusion

This study has shown the benefit of the employment of an inerter-based dynamic vibration absorber in a machining operation in terms of the machining chatter stability. An undamped system and four different configurations were employed for the simulations. The design parameters of the configurations were obtained via Self-adaptive Differential Evolution algorithm. It has been seen that the objective function of the optimisation must be the negative real part of the FRF to achieve the optimal parameters which give the best performance. Almost 37% improvement was achieved in a comparison to a traditional dynamic vibration absorber that is similarly tuned to maximise the chatter stability.

Acknowledgments

N.D. Sims and H. Dogan would like to acknowledge the support of EPSRC (grant EP/L016257/1).

Appendix A. Expressions for R_{ni}, R_{di}, I_{ni} and I_{di}

The full expression of the terms in Equation 14:

For $i = 1, ..., 4.$

$$
\begin{aligned}
R_{n1} =& -2\delta\eta^2\gamma^2\lambda^2\zeta + 2\eta^2\gamma^4\zeta - 2\eta^2\gamma^2\lambda^2\zeta - 2\gamma^2\lambda^2\zeta + 2\lambda^4\zeta \\
I_{n1} =& \delta\eta^2\gamma^3\lambda - \delta\eta^2\gamma\lambda^3 \\
R_{d1} =& 2\delta\eta^2\gamma^2\lambda^4\mu\zeta + 2\delta\eta^2\gamma^2\lambda^4\zeta - 2\eta^2\gamma^4\lambda^2\mu\zeta - 2\eta^2\gamma^4\lambda^2\zeta + 2\eta^2\gamma^2\lambda^4\zeta - 2\delta\eta^2\gamma^2\lambda^2\zeta \\
& + 2\gamma^2\lambda^4\mu\zeta + 2\eta^2\gamma^4\zeta - 2\eta^2\gamma^2\lambda^2\zeta + 2\gamma^2\lambda^4\zeta - 2\lambda^6\zeta - 2\gamma^2\lambda^2\zeta + 2\lambda^4\zeta \\
I_{d1} =& -\delta\eta^2\gamma^3\lambda^3\mu - \delta\eta^2\gamma^3\lambda^3 + \delta\eta^2\gamma\lambda^5 + \delta\eta^2\gamma^3\lambda - \delta\eta^2\gamma\lambda^3 \\
R_{n2} =& -\delta^2\eta^2\gamma^2\lambda^2 + \delta\eta^2\gamma^4 - \delta\eta^2\gamma^2\lambda^2 - \delta\gamma^2\lambda^2 + \delta\lambda^4 \\
I_{n2} =& -2\delta\gamma\lambda^3\zeta + 2\gamma^3\lambda\zeta - 2\gamma\lambda^3\zeta \\
R_{d2} =& \delta^2\eta^2\gamma^2\lambda^4\mu + \delta^2\eta^2\gamma^2\lambda^4 - \delta\eta^2\gamma^4\lambda^2\mu - \delta\eta^2\gamma^4\lambda^2 + \delta\eta^2\gamma^2\lambda^4 - \delta^2\eta^2\gamma^2\lambda^2 \\
& + \delta\gamma^2\lambda^4\mu + \delta\eta^2\gamma^4 - \delta\eta^2\gamma^2\lambda^2 + \delta\gamma^2\lambda^4 - \delta\lambda^6 - \delta\gamma^2\lambda^2 + \delta\lambda^4 \\
I_{d2} =& 2\delta\gamma\lambda^5\mu\zeta + 2\delta\gamma\lambda^5\zeta - 2\gamma^3\lambda^3\mu\zeta - 2\gamma^3\lambda^3\zeta + 2\gamma\lambda^5\zeta - 2\delta\gamma\lambda^3\zeta + 2\gamma^3\lambda\zeta - 2\gamma\lambda^3\zeta \\
R_{n3} =& \delta\eta^2\gamma^4 - \delta\eta^2\gamma^2\lambda^2 - \delta\gamma^2\lambda^2 + \delta\lambda^4 \\
I_{n3} =& 2\delta\eta^2\gamma^3\lambda\zeta - 2\delta\gamma\lambda^3\zeta + 2\gamma^3\lambda\zeta - 2\gamma\lambda^3\zeta \\
R_{d3} =& -\delta\eta^2\gamma^4\lambda^2\mu - \delta\eta^2\gamma^4\lambda^2 + \delta\eta^2\gamma^2\lambda^4 + \delta\gamma^2\lambda^4\mu + \delta\eta^2\gamma^4 - \delta\eta^2\gamma^2\lambda^2 + \delta\gamma^2\lambda^4 \\
& - \delta\lambda^6 - \delta\gamma^2\lambda^2 + \delta\lambda^4 \\
I_{d3} =& -2\delta\eta^2\gamma^3\lambda^3\mu\zeta - 2\delta\eta^2\gamma^3\lambda^3\zeta + 2\delta\gamma\lambda^5\mu\zeta + 2\delta\eta^2\gamma^3\lambda\zeta + 2\delta\gamma\lambda^5\zeta - 2\gamma^3\lambda^3\mu\zeta \\
& - 2\gamma^3\lambda^3\zeta + 2\gamma\lambda^5\zeta - 2\delta\gamma\lambda^3\zeta + 2\gamma^3\lambda\zeta - 2\gamma\lambda^3\zeta \\
R_{n4} =& -\delta^2\eta^2\gamma^2\lambda^2 + \delta\eta^2\gamma^4 - \delta\eta^2\gamma^2\lambda^2 - \delta\gamma^2\lambda^2 + \delta\lambda^4 \\
I_{n4} =& 2\delta\eta^2\gamma^3\lambda\zeta + 2\gamma^3\lambda\zeta - 2\gamma\lambda^3\zeta \\
R_{d4} =& \delta^2\eta^2\gamma^2\lambda^4\mu + \delta^2\eta^2\gamma^2\lambda^4 - \delta\eta^2\gamma^4\lambda^2\mu - \delta\eta^2\gamma^4\lambda^2 + \delta\eta^2\gamma^2\lambda^4 - \delta^2\eta^2\gamma^2\lambda^2 \\
& + \delta\gamma^2\lambda^4\mu + \delta\eta^2\gamma^4 - \delta\eta^2\gamma^2\lambda^2 + \delta\gamma^2\lambda^4 - \delta\lambda^6 - \delta\gamma^2\lambda^2 + \delta\lambda^4 \\
I_{d4} =& -2\delta\eta^2\gamma^3\lambda^3\mu\zeta - 2\delta\eta^2\gamma^3\lambda^3\zeta + 2\delta\eta^2\gamma^3\lambda\zeta - 2\gamma^3\lambda^3\mu\zeta - 2\gamma^3\lambda^3\zeta + 2\gamma\lambda^5\zeta \\
& + 2\gamma^3\lambda\zeta - 2\gamma\lambda^3\zeta
\end{aligned}
$$

References

[1] Tarngh Y S, Kao J Y and Lee E C 2000 Chatter suppression in turning operations with a tuned vibration absorber *Journal of Materials Processing Technology* **105** 55-60
[2] Moradi H, Bakhtiari-Nejad and Movahhedy M R 2008 Tuneable vibration absorber design to suppress vibrations: an application in boring manufacturing process *Journal of Sound and Vibration* **318** 93-108
[3] Wang M, Zan T, Yang Y and Fei R 2010 Design and implementation of nonlinear TMD for chatter suppression: an application in turning processes *International Journal of Machine Tools & Manufacture* **50** 474-479
[4] Yang Y, Dai W and Liu Q 2014 Design and implementation of two-degree-of-freedom tuned mass damper in milling variation mitigation *Journal Sound and Vibration* **335** 78-88
[5] Yang Y, Dai W and Liu Q 2017 Design and machining application of a two-DOF magnetic tuned mass damper *International Journal of Advanced Manufacturing Technology* **89** 1635-1643
[6] Yang Y, Munoa J and Altintas Y 2010 Optimization of multiple tuned mass dampers to suppress machine tool chatter *International Journal of Machine Tools and Manufacture* **50** 834-842
[7] Huyanan S 2007 An active vibration absorber for chatter reduction in machining *University of Sheffield PhD dissertation*
[8] Chung B, Smith S and Tlusty J 1997 Active damping of structural modes in high-speed machine tools *Journal of Vibration and Control* **3** 279-295
[9] Kuroda H, Arima F, Baba K and Inoue Y 2000 *12th World Conference on Earthquake Engineering* (Auckland) pp. 1-7
[10] Saito K, Yogo K, Sugimura Y, Nakaminami S and Park K 2004 *13th World Conference on Earthquake Engineering* (Vancouver) pp. 1764-1776
[11] Smith M C 2002 *Proceedings of the 41st IEEE Conference on Decision and Control* (Las Vegas) pp. 1657-1662
[12] Wang F C, Chen C W, Liao M K and Hong M F 2007 *Proceedings of the 46th IEEE Conference on Decision and Control* (New Orleans) pp. 3786-3791
[13] Lazar I F, Neild S A and Wagg D J 2014 Using an inerter-based device for structural vibration suppression *Earthquake Engineering and Structural Dynamics* **43** 1129-1147
[14] Jiang J Z, Matamoros-Sanchez A Z, Goodall R M and Smith M C 2012 Passive suspensions incorporating inerters for railway vehicles *Vehicle System Dynamics* **50** 263-276
[15] Smith M C and Wang F C 2004 Performance benefits in passive vehicle suspensions employing inerters *Vehicle System Dynamics* **42** 235-257
[16] Hu Y, Chen M Z Q and Shu Z 2014 Passive vehicle suspensions employing inerters with multiple performance requirements *Journal Sound and Vibration* **333** 2212-2225
[17] Wang F C and Lee C H 2018 *23rd International Symposium on Mathematical Theory of Networks and Systems* (Hong Kong) pp. 627-630
[18] Den Hartog J 1956 *Mechanical Vibrations* (New York: McGraw-Hill)
[19] Sims N D 2007 Vibration absorbers for chatter suppression: a new analytical tuning methodology *Journal Sound and Vibration* **301** 592-607
[20] Rubio L, Loya J A, Miguelez M H and Fernandez-Saez J 2013 Optimization of passive vibration absorbers to reduce chatter in boring *Mechanical Systems and Signal Processing* **41** 691-704
[21] Saravanamurugan S, Alwarsamy T and Devarajan K 2015 Optimization of damped dynamic vibration absorber to control chatter in metal cutting process *Journal of Vibration and Control* **21** 949-958
[22] Hu Y and Chen M Z Q 2015 Performance evaluation for inerter-based dynamic vibration absorbers *International Journal of Mec.* **99** 297-307
[23] Barredo E, Blanco A, Colin J, Penagos V M, Abundez A, Vela L G, Meza V, Cruz R H and Mayen J 2017 Closed-form solutions for the optimal design of inerter-based dynamic vibration absorbers *Journal of Mechanical Sciences* **144** 41-53
[24] Qin A and Sugantham P 2005 Self-adapative differential evolution algorithm for numerical optimization *2005 IEEE Congress on Evolutionary Computation* **2** 1785-1791